

Nitridocyanometalates of Cr^V, Mn^V, and Mn^{VI} †

Jesper Bendix, Karsten Meyer, Thomas Weyhermüller, Eckhard Bill, Nils Metzler-Nolte, and Karl Wieghardt*

Max-Planck-Institut für Strahlenchemie, D-45470 Mülheim an der Ruhr, Germany

Received October 31, 1997

Reaction of [Cr^V(N)(salen)]·CH₃NO₂ and [Mn^V(N)(salen)] in dimethylformamide or a methanol/water mixture with an aqueous solution of NaCN and CsCl or [N(CH₃)₄]Cl at elevated temperatures affords in good yields, respectively, yellow microcrystalline compounds of Cs₂Na[Cr^V(N)(CN)₅] (**1**); [N(CH₃)₄]₂Na[Cr^V(N)(CN)₅]·H₂O (**1a**) and pink-violet crystals of Cs₂Na[Mn^V(N)(CN)₅] (**4**); and [N(CH₃)₄]₂Na[Mn^V(N)(CN)₅]·H₂O (**4a**). These six-coordinate nitridopentacyanometalates contain a terminal M≡N unit and a labile cyano group in trans position. Recrystallization from water and addition of [PPh₄]Cl yields the five-coordinate species [PPh₄]₂[M(N)(CN)₄]·2H₂O (M = Cr^V (**2**), Mn^V (**5**)). From pyridine solutions of **2** and **5** the six-coordinate species [PPh₄]₂[M(N)(CN)₄(py)]·H₂O·py (M = Cr^V (**3**), Mn^V (**6**)) crystallize. Complexes **1**, **1a**, **2**, and **3** are paramagnetic (1.8 ± 0.1 μ_B at 298 K; d¹) whereas **4**, **4a**, **5**, and **6** have a low-spin d² ground state. Electrochemically, **5** can be reversibly one-electron-oxidized in CH₃CN with formation of a relatively stable [Mn^{VI}(N)(CN)₄]⁻ anion. Complexes **3**, **5**, and **6** have been characterized by single-crystal X-ray crystallography: **3** and **6** are isostructural and crystallize in the orthorhombic space group *Pnma* with *a* = 17.336(3) (17.254(3)) Å, *b* = 23.019(4) (22.873(4)) Å, *c* = 13.563(2) (13.490(2)) Å, *V* = 5412(2) (5324(2)) Å³, and *Z* = 4 (4) (values in parentheses refer to **6**); **5** crystallizes in the triclinic space group *P1̄* with *a* = 12.050(1), *b* = 12.310(1), *c* = 16.685(2) Å, α = 97.88(2)°, β = 109.33(2)°, γ = 90.55(2)°, *V* = 2309.4(4) Å³, and *Z* = 2. The complexes have been characterized by ¹³C and ¹⁵N NMR, UV–vis, EPR, IR/Raman, and MCD spectroscopies.

Introduction

High-valent nitrido complexes of chromium(V) and manganese(V) containing an M≡N structural motif are still a rather rare class of compounds.¹ This is mainly due to the fact that only a limited number of synthetic routes to such species appear to be available. Photolysis of azido chromium(III) and manganese(III) precursors (Arshankov reaction) is the most widely used method.² It has also been reported that treatment of Cr(III) and Mn(III) porphinato and *N,N'*-ethylenebis(salicylideneaminato) complexes with either NaOCl or PhIO in the presence of aqueous ammonia yields Cr^V≡N and Mn^V≡N species.^{3a–c} Cr(V) and Mn(V) nitridophthalocyaninato complexes have been obtained from [M^{III}(OH)₂Pc(2-)]⁻ (M = Cr, Mn) via oxidation in aqueous NH₃ solution with chlorine.^{3d,e} More recently, an efficient synthesis of Mn^V≡N species via oxidation of manganese(III) precursors in CH₂Cl₂/ammonia solution with *N*-bromosuccinimide was described.⁴

With one notable exception⁵ all complexes containing such an M≡N structural motif are five-coordinate with a square-based pyramidal coordination polyhedron where the nitrido ligand is in the apical position. The coligands employed are usually four-coordinate porphinato(2-), phthalocyaninato(2-), or *N,N'*-ethylenebis(salicylideneaminato)(2-) derivatives or two bidentate Schiff base ligands.⁶ These ligands display strong charge-transfer bands in the visible regions, and consequently, d–d transitions arising from the d¹ and d² electron configurations have not been readily identified or assigned.

In particular, it is somewhat surprising that simple nitridocyanometalates of Cr(V) and Mn(V) have not been described to date despite the fact that the corresponding analogues of Tc(V) and Re(V) are known. Thus [Tc^V(N)(CN)₄(OH₂)₂]²⁻, [Re^V(N)(CN)₄(OH₂)₂]²⁻, and [Re(N)(CN)₅]³⁻ have been synthesized and their tetraphenylphosphonium or -arsonium salts have been crystallographically characterized.^{7,8}

We have discovered that such species of Cr and Mn are readily synthesized by ligand substitution from solutions of [M(N)(salen)] (M = Cr^V, Mn^V)^{2b,9} to which an aqueous solution

† Dedicated to the memory of Professor Hans Siebert.

- (1) (a) Dehnicke, K.; Strähle, J. *Angew. Chem.* **1981**, *93*, 451; *Angew. Chem., Int. Ed. Engl.* **1981**, *20*, 414. (b) Dehnicke, K.; Strähle, J. *Angew. Chem.* **1992**, *104*, 978; *Angew. Chem., Int. Ed. Engl.* **1992**, *31*, 955. (c) Nugent, W. A.; Mayer, J. M. *Metal-Ligand Multiple Bonds*; Wiley-Interscience: New York, 1988.
- (2) (a) Arshankov, S. I.; Poznjak, A. L. *Zh. Neorg. Khim.* **1981**, *26*, 1576. (b) Arshankov, S. I.; Poznjak, A. L. *Z. Anorg. Allg. Chem.* **1981**, *481*, 201. (c) Bendix, J.; Wilson, S. R.; Prussak-Wiechowska, T. *Acta Crystallogr.*, in press.
- (3) (a) Buchler, J. W.; Dreher, C.; Lay, K.-L. *Z. Naturforsch., B: Anorg. Chem., Org. Chem.* **1982**, *37B*, 1155. (b) Hill, C. L.; Hollander, F. J. *J. Am. Chem. Soc.* **1982**, *104*, 7318. (c) Buchler, J. W.; Dreher, C.; Lay, K.-L.; Lee, Y. J. A.; Scheidt, W. R. *Inorg. Chem.* **1983**, *22*, 888. (d) Grunewald, H.; Homborg, H. *Z. Anorg. Allg. Chem.* **1992**, *608*, 81. (e) Grunewald, H.; Homborg, H. *Z. Naturforsch., B: Anorg. Chem., Org. Chem.* **1990**, *45B*, 483.

- (4) Du Bois, J.; Tomooka, C. S.; Hong, J.; Carreira, E. M.; Day, M. W. *Angew. Chem.* **1997**, *109*, 1722; *Angew. Chem., Int. Ed. Engl.* **1997**, *36*, 1645.
- (5) Niemann, A.; Bossek, U.; Haselhorst, G.; Wieghardt, K.; Nuber, B. *Inorg. Chem.* **1996**, *35*, 906.
- (6) Du Bois, J.; Tomooka, C. S.; Hong, J.; Carreira, E. M. *Acc. Chem. Res.* **1997**, *30*, 364.
- (7) Baldas, J.; Boas, J. F.; Colmanet, S. F.; Mackay, M. F. *Inorg. Chim. Acta* **1990**, *170*, 233.
- (8) (a) Purcell, W.; Potgieter, I. Z.; Damoense, L. J.; Leipoldt, J. G. *Transition Met. Chem.* **1991**, *16*, 473. (b) Purcell, W.; Potgieter, I. Z.; Damoense, L. J.; Leipoldt, J. G. *Transition Met. Chem.* **1992**, *17*, 387. (c) Britten, J. F.; Lock, C. J. L.; Wei, Y. *Acta Crystallogr., Sect. C*, **1993**, *C49*, 1280.

of NaCN has been added (salen = *N,N'*-ethylenebis(salicylideneamino)). Here we report the preparations and molecular and electronic structures of nitridocyanometalates of Cr^V, Mn^V, and Mn^{VI}.

Experimental Section

The ligand salenH₂¹⁰ and the complexes [Cr^{III}(N₃)(salen)H₂O]^{2b} and [Mn^V(N)(salen)]⁹ were prepared according to literature methods.

[Cr^V(N)(salen)]·CH₃NO₂ was prepared by a modification of the procedure reported by Arshankov and Poznjak.^{2b,c}

Cs₂Na[Cr^V(N)(CN)₅] (1). To a solution of [Cr^V(N)(salen)]·CH₃NO₂ (0.21 g; 0.60 mmol) in DMF (9 mL) was added an aqueous solution (8 mL) of NaCN (2.0 g; 40.8 mmol) and CsCl (1.0 g; 5.9 mmol). The resulting solution was heated to reflux for 20 min in the dark and then cooled to 5 °C. The bright-yellow crystals that precipitated were collected by filtration, washed with methanol, and air-dried. Yield: 0.20 g (70%). Anal. Calcd for C₅N₆NaCrCs₂: C, 12.39; N, 17.33; Cr, 10.72. Found: C, 12.29; N, 17.05; Cr, 11.16.

[N(CH₃)₄]₂Na[Cr^V(N)(CN)₅]·H₂O (1a). This salt was prepared as described above for **1** by using [N(CH₃)₄]Cl (2.0 g) instead of CsCl. Yield: 0.13 g (57%). Anal. Calcd for C₁₃H₂₆N₈ONaCr: C, 40.52; H, 6.80; N, 29.08; Na, 5.97; Cr, 13.49. Found: C, 40.76; H, 6.20; N, 29.28; Na, 5.95; Cr, 13.46.

[PPh₄]₂[Cr^V(N)(CN)₄]·2H₂O (2). A solution of **1a** (0.10 g; 0.21 mmol) in water (6.5 mL) was allowed to slowly diffuse through a glass frit into a solution of [PPh₄]Cl (0.20 g; 0.53 mmol) in water (15 mL). The pale yellow crystals that precipitated were collected by filtration, washed with water, and air-dried. Yield: 0.16 g (86%). Anal. Calcd for C₅₂H₄₄N₅O₂P₂Cr: C, 70.58; H, 5.01; N, 7.91; Cr, 5.88. Found: C, 70.85; H, 4.83; N, 7.80; Cr, 5.96. ESI (electrospray ionization mass spectrometry; negative ion detection): *m/z* = 509 {[PPh₄][Cr(N)(CN)₄]}⁻.

[PPh₄]₂[Cr^V(N)(CN)₄(py)]·H₂O·py (3). Recrystallization of **2** (0.18 g; 0.21 mmol) from pyridine (py) solution (3 mL) at 5 °C gave yellow crystals of **3**. Yield: 0.11 g (53%). Anal. Calcd for C₆₂H₅₂CrN₇OP₂: C, 72.65; H, 5.11; N, 9.56; Cr, 5.07. Found: C, 72.45; H, 5.02; N, 9.63; Cr, 5.30.

Cs₂Na[Mn^V(N)(CN)₅] (4) and [N(CH₃)₄]₂Na[Mn^V(N)(CN)₅]·H₂O (4a). To a suspension of [Mn^V(N)(salen)] (2.5 g; 7.1 mmol) in a water/methanol mixture (125 mL and 25 mL, respectively) was added NaCN (11.0 g; 224.4 mmol). After the mixture was heated to reflux for 1 h, [N(CH₃)₄]Cl (18.0 g; 164.2 mmol) was added to the dark red solution, which was filtered hot. Upon cooling of the filtrate to 5 °C, pink-violet crystals precipitated. Yield: 1.75 g (64%). Anal. Calcd for C₁₃H₂₆N₈ONaMn: C, 40.21; H, 6.75; N, 28.86; Na, 5.92; Mn, 14.15. Found: C, 40.15; H, 6.66; N, 28.79; Na, 6.3; Mn, 14.10.

To a solution of the above crystals (0.40 g; 1.03 mmol) and NaCN (0.20 g; 4.1 mmol) in water (12 mL) was added a solution of CsCl (1.0 g) in water (15 mL). A pink-violet precipitate of Cs₂Na[Mn(N)(CN)₅] formed immediately in quantitative yield. Anal. Calcd for C₅N₆NaMnCs₂: C, 12.31; N, 17.23; Mn, 11.26. Found: C, 12.14; N, 17.46; Mn, 10.73.

[PPh₄]₂[Mn^V(N)(CN)₄]·2H₂O (5). To a solution of **4a** (0.275 g; 0.56 mmol) and NaCN (0.10 g; 2.04 mmol) in water (7 mL) was slowly added a solution of [PPh₄]Cl (0.60 g; 1.60 mmol) in water (10 mL). Orange-pink needles of **5** precipitated immediately. Yield: 0.46 g (73%). Anal. Calcd for C₅₂H₄₄N₅O₂P₂Mn: C, 70.35; H, 5.00; N, 7.89; Mn, 6.19. Found: C, 69.88; H, 5.03; N, 7.96; Mn, 6.28. ESI—negative ion: *m/z* = 512 {[PPh₄][Mn(N)(CN)₄]}⁻.

[PPh₄]₂[Mn^V(N)(CN)₄(py)]·H₂O·py (6). Recrystallization of **5** (0.24 g; 0.27 mmol) from pyridine (4.0 mL) as described above for **3** afforded crystalline **6** in 61% yield. Anal. Calcd for C₆₂H₅₂N₇OP₂Mn: C, 72.44; H, 5.10; N, 9.54; Mn, 5.34. Found: C, 70.69; H, 5.34; N, 9.38; Mn, 5.22.

Physical Measurements. NMR spectra were recorded on Bruker DRX 400 and DRX 500 instruments at 100.62 MHz/125.77 MHz (¹³C) and 50.7 MHz (¹⁵N) at room temperature. ¹³C NMR spectra were

Table 1. Crystallographic Data for the Complexes

	3	5	6
formula	C ₆₂ H ₅₄ CrN ₇ OP ₂	C ₅₂ H ₄₄ MnN ₅ O ₂ P ₂	C ₆₂ H ₅₄ MnN ₇ OP ₂
fw	1027	887.8	1030
space group	<i>Pnma</i>	<i>P</i> $\bar{1}$ (No. 2)	<i>Pnma</i>
temp, K	100(2)	100(2)	100(2)
λ , Å	0.710 73	0.710 73	0.710 73
<i>a</i> , Å	17.336(3)	12.050(1)	17.254(3)
<i>b</i> , Å	23.019(4)	12.310(1)	22.873(4)
<i>c</i> , Å	13.563(2)	16.685(2)	13.490(2)
α , deg	90	97.88(2)	90
β , deg	90	109.33(2)	90
γ , deg	90	90.55(2)	90
<i>V</i> , Å ³	5412(2)	2309.4(4)	5324(2)
<i>Z</i>	4	2	4
ρ_{calc} , g cm ⁻³	1.260	1.277	1.285
$\mu(\text{Mo K}\alpha)$, mm ⁻¹	0.319	0.401	0.357
<i>R</i> ₁ ^a	0.042	0.036	0.056
<i>wR</i> ₂ ^b	0.091	0.089	0.103

^a $R_1 = \sum ||F_o| - |F_c|| / \sum |F_o|$ for $F_o^2 > 2\sigma(F_o^2)$. ^b $wR_2 = \{ \sum [w(F_o^2 - F_c^2)^2] / \sum [w(F_o^2)^2] \}^{1/2}$ for $F_o^2 > 2\sigma(F_o^2)$.

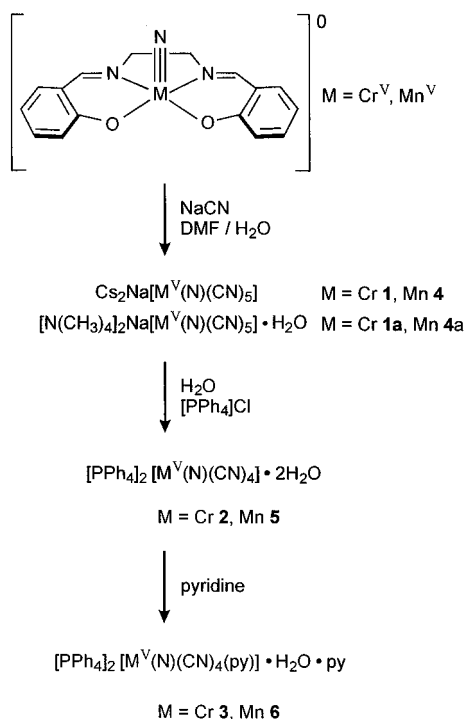
referenced internally to the solvent signal, and ¹⁵N spectra, externally to the absolute frequency of 50.696 991 0 MHz, which was the resonance frequency of neat nitromethane under the same experimental conditions ($\delta(^{15}\text{N})$ (CH₃NO₂) = 0 ppm). ¹⁵N NMR spectra were recorded in 5 mm tubes with a triple-resonance indirect-detection ¹H/¹⁵N/broad-band probe. Instead of the dedicated ¹⁵N coil, the broad-band coil was used for ¹⁵N detection in order to reduce interference with the lock signal (90° pulse: 16 μ s at full power). Samples were 50% ¹⁵N labeled at the terminal nitrido group¹¹ (~5 mg sample in 0.5 mL of solvent). Using 30° pulses, a ¹⁵N signal was, in general, detected after ~300 scans. The signal from CD₃CN ($\delta = -136$ ppm) was much stronger in intensity than the signal of the sample, and it was used to check the scale of the spectrum and to verify that the nitrido signal was not folded. Electronic spectra were recorded on a Perkin-Elmer Lambda 19 (range: 220–1400 nm) spectrophotometer. Cyclic voltammetry and coulometry were performed with EG & G equipment (model 273 A potentiostat/galvanostat). X-band EPR spectra of the complexes were recorded on a Bruker ESP 300 E spectrometer equipped with an Oxford Instruments ESR 910 helium-flow cryostat. Simulations of the spectra were performed by using the Simfonia program (Bruker) and by use of the EPR simulation program package written by Weihe.^{12a} Infrared and Raman ($\lambda = 1064$ nm) spectra were recorded on solid samples (KBr disks) on a Perkin-Elmer 2000 FT-IR/FT-NIR Raman spectrometer. The MCD spectra were recorded at room temperature in acetonitrile on a Jasco J-710/720 spectropolarimeter equipped with an electromagnet providing a magnetic field of 1.6 T. The samples were measured with the field parallel and antiparallel to the light propagation direction, and the differences of these measurements are reported, thus giving an effective applied field of 3.2 T.

X-ray Crystallography. Crystal data and data collection and refinement details are summarized in Table 1 (and corresponding tables in the Supporting Information). Graphite-monochromated Mo K α X-radiation was used throughout. Intensities of an orange-yellow crystal of **3** and pink-violet crystals of **5** and **6** were collected at 100(2) K by using the Siemens SMART system; they were corrected for Lorentz and polarization effects and corrected for absorption by using the SADABS program (G. M. Sheldrick, Universität Göttingen). The structures were solved by conventional Patterson and difference Fourier methods by using the Siemens SHELXTL-PLUS program package.^{12b} The function minimized during full-matrix least-squares refinement was

- (11) At the nitrido group, ¹⁵N-labeled isotopomers of **4–6** were prepared by ligand displacement from {[Mn(^{14/15}N)(cyclam)]₂(μ -N₃)}(ClO₄)₃ with aqueous NaCN. This species was prepared by photolysis of [Mn^{III}(N₃)₂(cyclam)](ClO₄) into which [¹⁴N–¹⁴N–¹⁵N]⁻ was introduced. The resulting Mn≡N species contain 50% Mn≡¹⁴N and 50% Mn≡¹⁵N isotopomers. Details of this chemistry will be published elsewhere.
 (12) (a) Glerup, J.; Weihe, H. *Acta Chem. Scand.* **1991**, *45*, 444. (b) Sheldrick, G. M. Full-matrix least-squares refinement package SHELXTL-PLUS. Universität Göttingen, 1991.

(9) Du Bois, J.; Hong, J.; Carreira, E. M.; Day, M. W. *J. Am. Chem. Soc.* **1996**, *118*, 915.

(10) Mason, A. T. *Chem. Ber.* **1887**, *20*, 267.

Scheme 1. Syntheses of Complexes and Labeling Scheme

$\sum w(|F_o| - |F_c|)^2$. All non-hydrogen atoms were refined anisotropically. The C–H hydrogen atoms were placed at calculated positions with isotropic thermal parameters. The O–H hydrogen atoms were located in the difference Fourier map and were readily refined with isotropic thermal parameters.

Results

Syntheses of Complexes. The synthetic routes employed and complexes prepared are summarized in Scheme 1. When solutions of $[\text{Cr}(\text{N})(\text{salen})] \cdot \text{CH}_3\text{NO}_2$ or $[\text{Mn}(\text{N})(\text{salen})]$ in dimethylformamide (DMF) were treated with an aqueous solution of a large excess of NaCN and CsCl or $[\text{N}(\text{CH}_3)_4]\text{Cl}$ and heated to reflux in the absence of light, a bright-yellow precipitate of $\text{Cs}_2\text{Na}[\text{Cr}^{\text{V}}(\text{N})(\text{CN})_5]$ (**1**) or $[\text{N}(\text{CH}_3)_4]_2\text{Na}[\text{Cr}^{\text{V}}(\text{N})(\text{CN})_5]$ (**1a**) or, alternatively, of pink $\text{Cs}_2\text{Na}[\text{Mn}^{\text{V}}(\text{N})(\text{CN})_5]$ (**4**) and $[\text{N}(\text{CH}_3)_4]_2\text{Na}[\text{Mn}^{\text{V}}(\text{N})(\text{CN})_5] \cdot \text{H}_2\text{O}$ (**4a**) formed in 50–70% yield based on the salen starting materials. These complexes contain the distorted octahedral C_{4v} symmetric ion $[\text{M}(\text{N})(\text{CN})_5]^{3-}$ where $\text{M} = \text{Cr}^{\text{V}}, \text{Mn}^{\text{V}}$.

The cyano ligand in trans position relative to the $\text{M} \equiv \text{N}$ group in **1**, **1a**, **4**, and **4a** is labile and dissociates in aqueous solution with formation of the two five-coordinate $[\text{M}(\text{N})(\text{CN})_4]^{2-}$ species ($\text{M} = \text{Cr}, \text{Mn}$) which were isolated as tetraphenylphosphonium salts, i.e., yellow $[\text{PPh}_4]_2[\text{Cr}^{\text{V}}(\text{N})(\text{CN})_4] \cdot 2\text{H}_2\text{O}$ (**2**) and orange-pink $[\text{PPh}_4]_2[\text{Mn}^{\text{V}}(\text{N})(\text{CN})_4] \cdot 2\text{H}_2\text{O}$ (**5**).

Recrystallization of **2** and **5** from neat pyridine was found to produce the pseudooctahedral anions $[\text{M}(\text{N})(\text{CN})_4(\text{py})]^{2-}$, which were isolated as yellow $[\text{PPh}_4]_2[\text{Cr}(\text{N})(\text{CN})_4(\text{py})] \cdot \text{H}_2\text{O} \cdot \text{py}$ (**3**) and violet $[\text{PPh}_4]_2[\text{Mn}(\text{N})(\text{CN})_4(\text{py})] \cdot \text{H}_2\text{O} \cdot \text{py}$ (**6**) where py represents pyridine. Upon prolonged standing of **3** and **6** in air at ambient temperature, the crystals lose the pyridine molecules. The chromium(V) complexes **1**, **1a**, **2**, and **3** were found to be light-sensitive even in the solid state. Figure 1 shows the infrared and Raman spectra of solid **4** which consist of the $\text{Mn} \equiv ^{14}\text{N}$ $\text{Mn} \equiv ^{15}\text{N}$ isotopomers in a 1:1 ratio.¹¹ Table 2 summarizes the corresponding spectra of **1–6**. In each case the $\nu(\text{C} \equiv \text{N})$ stretching mode has been identified in the narrow range 2110–2145 cm^{-1} .

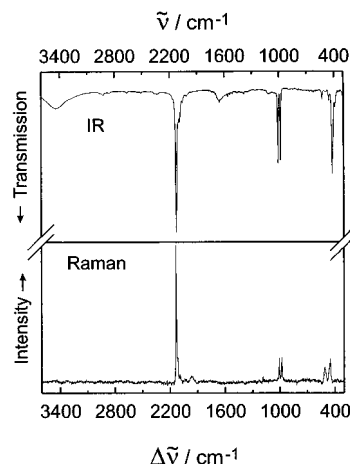


Figure 1. Infrared (top) and Raman (bottom) spectra of an isotomeric mixture (1:1) of solid $\text{Cs}_2\text{Na}[\text{Mn}^{(14/15)\text{N}}(\text{CN})_5]$ (KBr disks).

The $\nu(\text{M} \equiv \text{N})$ stretching mode for $\text{Cr} \equiv \text{N}$ species is sensitive to the presence or absence of a coordinated ligand in trans position. Thus, for the five-coordinate species **2**, this mode is observed at 1052 cm^{-1} whereas, for the six-coordinate species **1** and **3**, it is at 972 and 995 cm^{-1} , respectively. Similarly, species containing the $\text{Mn} \equiv \text{N}$ moiety display this vibration at 1011 cm^{-1} for **4** and 1041 cm^{-1} for **6**, where both species are six-coordinate, whereas for **5**—a five-coordinate complex—the $\nu(\text{Mn} \equiv ^{14}\text{N})$ stretch is observed at 1094 cm^{-1} . In the cases of **4** and **5**, these assignments are corroborated by the spectra of the $\text{Mn} \equiv ^{15}\text{N}$ isotopomers.¹¹ A shift of the $\nu(\text{Mn} \equiv ^{15}\text{N})$ mode to lower frequencies by approximately 25 cm^{-1} is in excellent agreement with a harmonic oscillator model (calculated: 27 cm^{-1}).

Room-temperature effective moments of $1.8 \pm 0.1 \mu_{\text{B}}$ for complexes **1**, **1a**, **2**, and **3** are in excellent agreement with a d^1 electron configuration for Cr^{V} . In contrast, the Mn^{V} complexes **4**, **4a**, **5**, and **6** with a d^2 electron configuration display a significant temperature-independent paramagnetism in the range 100–300 K (~ 0.3 – $0.4 \mu_{\text{B}}$ at 298 K). At temperatures < 100 K the molar magnetic susceptibility increases with decreasing temperature, indicating the presence of small paramagnetic impurities ($\sim 1\%$). Thus the d^2 electrons are paired in these complexes.

Crystal Structures. The structures of **3**, **5**, and **6** have been determined by single-crystal X-ray crystallography at 100(2) K. Selected bond distances and angles are summarized in Table 3, Figure 2 shows the structure of the complex anion in crystals of **3**, and Figure 3 shows the anion in crystals of **5**.

Complexes **3** and **6** are isostructural; they consist of well-separated $[\text{PPh}_4]^+$ cations, the anions $[\text{M}(\text{N})(\text{CN})_4(\text{py})]^{2-}$ ($\text{M} = \text{Cr}^{\text{V}}, \text{Mn}^{\text{V}}$), and molecules of water and pyridine of crystallization. The anions $[\text{M}(\text{N})(\text{CN})_4(\text{py})]^{2-}$ possess a severely distorted octahedral coordination polyhedron comprising four cyano ligands in an equatorial plane, a terminal nitrido, and a coordinated pyridine in trans position relative to the $\text{M} \equiv \text{N}$ moiety. The $\text{Cr} \equiv \text{N}$ and $\text{Mn} \equiv \text{N}$ bond lengths at 1.570(3) and 1.525(4) Å, respectively, are very short and indicate triple-bond character. In contrast, the $\text{M}-\text{N}_{\text{py}}$ distances are very long (2.542(4) Å in **3**, 2.472(4) Å in **6**). The four $\text{M}-\text{C}$ distances in each anion are within experimental error identical; the averaged values are 2.078(5) Å in **3** and 1.997(5) Å in **6**. Both anions are bisected by a crystallographic mirror plane; the MC_4N_2 polyhedra possess idealized C_{4v} symmetry. The Cr^{V} and Mn^{V} ions in **3** and **6** are not located in the equatorial plane defined by the four carbon atoms of the cyano ligands; the Cr^{V}

Table 2. IR and Raman Spectroscopic Data^a

complex	$\nu(\text{M}\equiv\text{N}), \text{cm}^{-1}$		$\nu(\text{C}\equiv\text{N}), \text{cm}^{-1}$		$\delta(\text{M}-\text{CN}), \text{cm}^{-1}$	
	IR	Raman	IR	Raman	IR	Raman
1	972	974	2141, 2111	2140, 2113	484	484
2	1052	1044	2130	2132		
3	995	999	2131, 2122	2129, 2120		
4	1011 (986)	1011 (981)	2127	2140, 2132	425, 411	(512, 454)
5	1094 (1065)	1085 (1062)	2126, 2115	2131, 2120		
6 [Ti(CN) ₆] ³⁻ ^b	1041		2121, 2114 2071		390	

^a Solid-state spectra (KBr disks); values in parentheses are for $\text{M}\equiv^{15}\text{N}$ isotopomers. ^b Reference 18.

Table 3. Selected Bond Distances (Å) and Angles (deg) of the Anions in **3**, **5**, and **6**

Complex 3 (M = Cr) and in Parentheses 6 (M = Mn)			
M–N10	1.570(3) (1.525(4))	M–C2	2.078(4) (1.997(5))
M–N4	2.542(4) (2.472(4))	M–C3	2.080(2) (1.994(3))
M–C1	2.077(4) (2.001(5))	C1–N1	1.162(4) (1.156(5))
C2–N2	1.159(4) (1.157(6))	C3–N3	1.155(3) (1.158(3))
N10–M–C1	99.3(1) (98.8(2))	N10–M–C2	96.7(1)
C1–M–C2	164.0(1) (164.1(2))	C2–M–C3	90.59(6) (90.1(1))
C1–M–C3	87.63(6) (88.2(1))	N2–C2–M	178.7(3) (178.2(4))
N10–M–C3	96.42(6) (96.2(1))		
N1–C1–M	178.2(3) (178.4(4))		
N3–C3–M	176.2(2) (177.0(3))		
Complex 5			
Mn–N10	1.507(2)	Mn–C4	1.974(2)
Mn–C2	1.976(2)	Mn–C1	1.985(2)
Mn–C3	1.995(2)	C1–N1	1.162(2)
C2–N2	1.160(2)	C3–N3	1.159(2)
N10–Mn–C4	105.7(1)	N10–Mn–C2	105.1(1)
C4–Mn–C2	149.0(1)	N10–Mn–C1	100.4(1)
C4–Mn–C1	85.4(1)	C2–Mn–C1	86.9(1)
N10–Mn–C3	99.7(1)	C4–Mn–C3	87.5(1)
C2–Mn–C3	89.6(1)	C1–Mn–C3	159.9(1)
N1–C1–Mn	177.3(2)	N2–C2–Mn	176.1(2)

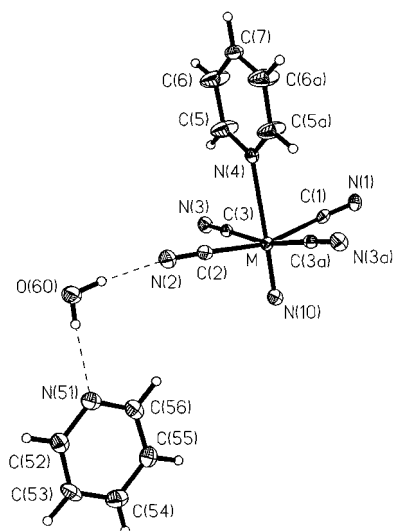


Figure 2. Perspective view of the $[\text{Mn}^{\text{V}}(\text{N})(\text{CN})_4(\text{py})]^{2-}$ anion in conjunction with the hydrogen bonding of the water and pyridine molecules of crystallization in crystals of **6** (M = Mn). The view of the corresponding anion, H_2O , and pyridine molecules in crystals of **3** (M = Cr) is very similar and is not shown. (Small open circles represent hydrogen atoms.)

ion in **3** lies 0.261(2) Å and the Mn^{V} ion in **6** lies 0.246(2) Å above this best plane. In the solid state, the water molecule of crystallization forms weak hydrogen-bonding contacts to one of the cyano groups of the anions and to the nitrogen of the pyridine molecule of crystallization ($\text{O}(60)\cdots\text{N}(2) = 2.933(6)$

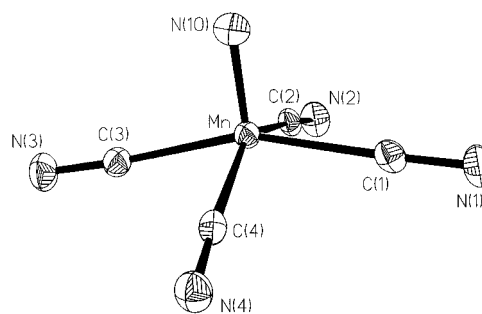


Figure 3. Perspective view of the five-coordinate anion $[\text{Mn}(\text{N})(\text{CN})_4]^{2-}$.

and 2.914(5) Å and $\text{O}(60)\cdots\text{N}(51) = 2.859(6)$ and 2.842(5) Å in **3** and **6**, respectively) but not to the nitrido group.

The structure of **5** consists of well-separated $[\text{PPh}_4]^+$ cations and $[\text{Mn}(\text{N})(\text{CN})_4]^{2-}$ anions and water molecules of crystallization. The five-coordinate anion possesses a square-based pyramidal coordination polyhedron with a terminal nitrido ligand in apical position. The $\text{Mn}\equiv\text{N}$ bond at 1.507(2) Å is extremely short. The Mn^{V} ion lies 0.436 Å above the equatorial plane defined by the four carbon atoms of the coordinated cyano groups. The average $\text{Mn}-\text{C}$ bond distance at 1.982 Å is slightly shorter than that in the six-coordinate anion of **6**.

Interestingly, the two water molecules of crystallization are not located in the vicinity of the vacant sixth coordination site of the anion; instead they form weak intermolecular hydrogen-bonding contacts ($\text{N}(1)\cdots\text{O}(10) = 2.972(4)$ Å, $\text{N}(3)\cdots\text{O}(20) = 3.049(5)$ Å) to two nitrogen atoms of two cyano groups as is schematically depicted in Figure 4. The anions and water molecules form an infinite chain structure in the solid state.

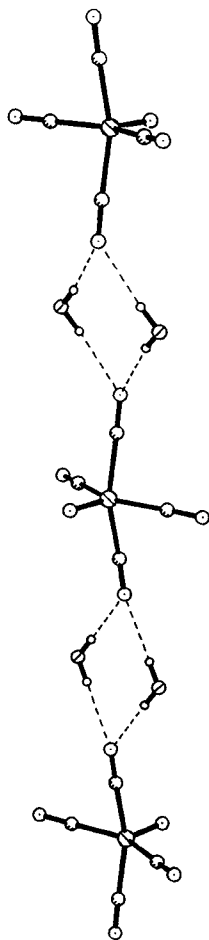


Figure 4. Ball-and-stick representation of the infinite-chain structure of the anions in crystals of **5**.

Again, the terminal nitrido group is not involved in any hydrogen bonding.

Electrochemistry. Cyclic voltammograms of **2** and **5** have been recorded in acetonitrile solution (0.10 M [N(*n*-butyl)₄]PF₆ supporting electrolyte) at a glassy carbon working electrode at ambient temperature. All potentials are referenced versus the ferrocenium/ferrocene (Fc⁺/Fc) couple. In the potential range -1.0 to +1.8 V, complex **2** does not display any redox activity. In contrast, complex **5** exhibits a reversible one-electron-transfer wave at $E_{1/2} = 0.496$ V ($\Delta(E^{p_{ox}} - E^{p_{red}}) \sim 75$ mV, $I_{ox}/I_{red} = 1.09$ at 100 mV s⁻¹ scan rate) using the same experimental conditions. Coulometric measurements (three successive experiments: oxidation, reduction, and reoxidation) prove that **5** can be one-electron oxidized on the time scale of such an experiment without noticeable decomposition as depicted in eq 1. Thus the Mn^{VI} oxidation level is electrochemically accessible.



¹³C and ¹⁵N NMR Spectroscopy. ¹³C and ¹⁵N NMR spectra of samples ¹⁵N-labeled (50%) at the terminal nitrido group of **4** (solvent D₂O, 0.1 M NaCN), **5** (CD₃CN), and **6** (CD₃CN) were recorded at ambient temperature; the results are summarized in Table 4.

For the three samples, one ¹⁵N signal of the terminal nitrido group only and one ¹³C signal of the cyano groups was observed, respectively. Two aspects of these data deserve a comment. First, the ¹⁵N NMR spectra display a signal in the range $\delta = 629$ –688 ppm, contrasting in this respect with second- and third-

Table 4. ¹⁵N and ¹³C Chemical Shifts of the Complexes^a

complex	δ , ppm		solvent	ref
	¹⁵ N NMR	¹³ C NMR		
5	629.0	148.58	CD ₃ CN	this work
6	645.4	151.07	D ₂ O	this work
4	687.6	156.61	CD ₃ CN	this work
[Mo(¹⁵ N)(S ₂ CNEt ₂) ₃]	40.0		CH ₂ Cl ₂	13a
<i>trans</i> -[MoBr(¹⁵ N)(dppe) ₂]	190.6		thf	13b
[ReCl(¹⁵ N)(dppe) ₂]Cl	67.1		CH ₂ Cl ₂	13a

^a dppe = Ph₂PCH₂CH₂PPh₂.

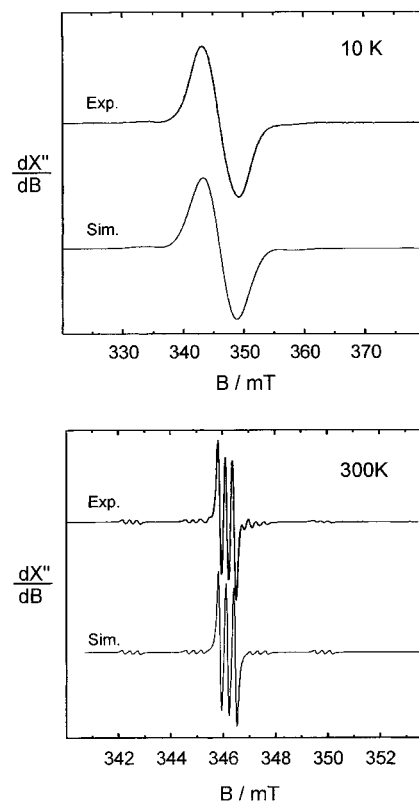


Figure 5. X-band and EPR spectra of an acetonitrile solution of **2** at 300 and 10 K and simulations (for parameters, see text). (Conditions: 9.6474 GHz, modulation amplitude 0.14 G.)

row transition metal ion nitrido complexes which have chemical shifts in the range 40–200 ppm.¹³ Thus the observed chemical shifts of the Mn≡¹⁵N unit exceed all reported values and indicate an enormous deshielding of the nitrido nucleus. This agrees nicely with the lacking nucleophilicity or basicity of this terminal Mn≡N group. Second, the parallel deshielding of the ¹³C and ¹⁵N nuclei in **5**, **6**, and **4** is a function of the presence or absence of a ligand *trans* to the Mn≡N group; furthermore, a cyano group is a better π -acceptor than pyridine and, consequently, the deshielding increases.

EPR Spectroscopy. We have recorded the X-band EPR spectra of **2** and the electrochemically oxidized form of **5** in acetonitrile at 300 and 10 K, respectively. Spectra of **2** are shown in Figure 5 whereas those of [Mn^{VI}(N)(CN)₄]⁻ are shown in Figure 6. The spectra have been successfully simulated.

The spectrum of **2** at 300 K shows one group of three lines stemming from the ^{50,52,54}Cr nuclei ($I = 0$) (90.5% natural abundance) and four groups of three lines from ⁵³Cr ($I = 3/2$) (9.5% natural abundance). The splitting into three lines for each

(13) (a) Dilworth, J. R.; Donovan-Mtunzi, S.; Kan, C. T.; Richards, R. L. *Inorg. Chim. Acta* **1981**, 53, L161. (b) Donovan-Mtunzi, S.; Richards, R. L.; Mason, J. J. *Chem. Soc., Dalton Trans.* **1984**, 1329.

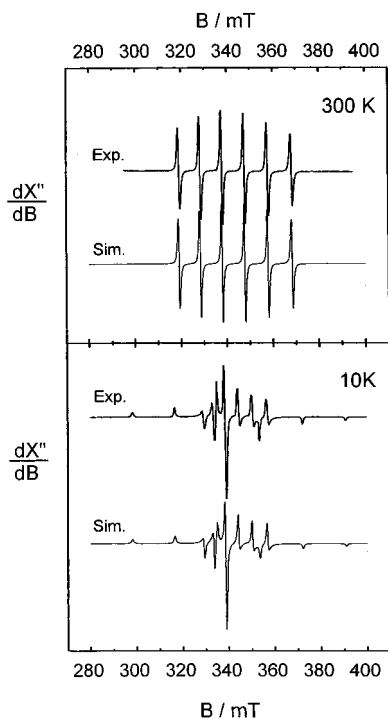


Figure 6. X-band and EPR spectra of electrochemically generated $[\text{Mn}^{\text{VI}}(\text{N})(\text{CN})_4]^-$ in CH_3CN (0.10 M $[\text{N}(n\text{-butyl})_4]\text{PF}_6$) at 300 K (top) and 10 K (bottom) and simulations using parameters given in the text. (Condition: 9.6474 GHz.)

resonance is due to superhyperfine coupling to a single nitrogen ($I = 1$). Coupling constants of $A(^{53}\text{Cr}) = 22.8 \times 10^{-4} \text{ cm}^{-1}$ and $A(^{14}\text{N}) = 2.73 \times 10^{-4} \text{ cm}^{-1}$ have been obtained. The ^{14}N superhyperfine coupling constant agrees well with values reported for $[\text{Cr}^{\text{V}}(\text{N})(\text{L}^1)]$, $[\text{Cr}^{\text{V}}(\text{N})(\text{ttp})]$, and $[\text{Cr}^{\text{V}}(\text{N})(\text{oep})]$ where L^1 represents N,N' -bis(pyridine-2-carbonyl)-*o*-phenylenediamide(2-), ttp is tetratolylporphinate(2-) and oep is octaethylporphinate(2-).¹⁴ At 10 K in frozen CH_3CN solution, the spectrum has no resolved hyperfine structure ($g = 1.9920$; $A(^{53}\text{Cr}) = 60 \times 10^{-4} \text{ cm}^{-1}$).

The spectrum of $[\text{Mn}^{\text{VI}}(\text{N})(\text{CN})_4]^-$ in CH_3CN at 300 K displays a typical six-line isotropic spectrum (^{55}Mn ; $I = 5/2$) at $g = 2.003$ and $A(^{55}\text{Mn}) = 92 \times 10^{-4} \text{ cm}^{-1}$ whereas at 10 K an axial spectrum is observed at $g_{zz} = 1.999$, $g_{xx} = g_{yy} = 2.0045$, $A_{zz} = 173.7 \times 10^{-4} \text{ cm}^{-1}$, and $A_{xx} = A_{yy} = 51.10 \times 10^{-4} \text{ cm}^{-1}$, in excellent agreement with the d^1 electron configuration of a C_{4v} symmetric Mn(VI) ion. A similar isotropic spectrum at 295 K has been reported for the only other characterized tetrahedral Mn^{VI} complex¹⁵ ($A(^{55}\text{Mn}) = 59\text{G}$, $g = 2.004$).

Electronic Spectra. Table 5 summarizes the electronic spectra of complexes.

The UV-vis spectra of **1a** and **4a** in 1.0 or 0.1 M aqueous NaCN solution are shown in Figure 7. Under these conditions the $[\text{M}(\text{N})(\text{CN})_5]^{3-}$ anions are the prevalent species. The anions possess C_{4v} symmetry. When the spectra are recorded in pure water as solvent, ligand dissociation generates the $[\text{M}(\text{N})(\text{CN})_4]^{2-}$ anions (also C_{4v} symmetry). Thus the spectra of **4a** in H_2O and **5** in acetonitrile are very similar in the visible region. The

Table 5. Electronic Spectral Data for the Complexes

complex	solvent	λ_{max} , nm (ϵ , $\text{L mol}^{-1} \text{ cm}^{-1}$)
1a	1 M NaCN	279 (3.15×10^3), 361 (104), 430 sh (30)
	H_2O	272 (2.54×10^3), 354 (140), 420 sh (60)
2	CH_3CN	see Figure 8
4a	0.1 M NaCN	287 (1.08×10^3), 370 sh (50), 516 (36)
	H_2O	287 (43), 370 sh (55), 493 (43)
5	CH_3CN	351 (40), 495 (55)
6	pyridine	366 (80), 507 (48)
	$[\text{Mn}^{\text{VI}}(\text{N})\text{-(CN)}_4]^-$	318 (3.27×10^3), 418 (1.73×10^3), 442 (1.43×10^3), 490 sh (1.0×10^3)

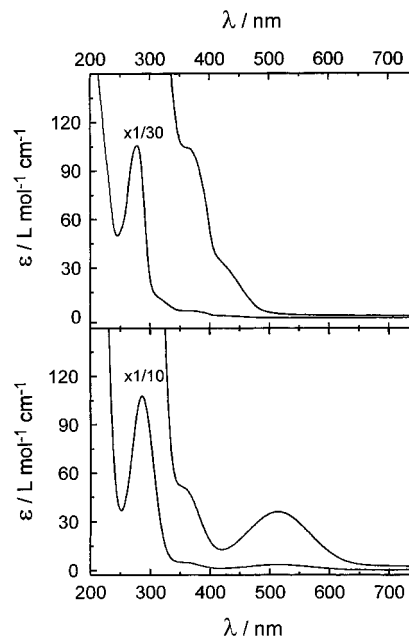


Figure 7. UV-vis spectra of **1a** (top) and **4** (bottom) in 1.0 and 0.1 M aqueous NaCN solution, respectively.

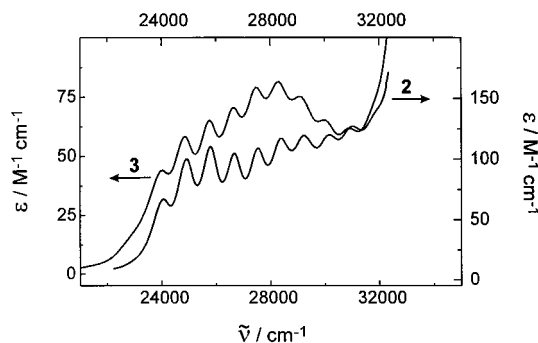


Figure 8. UV-vis spectra of **2** in acetonitrile and of **3** in pyridine.

spectrum of **5** displays $\pi \rightarrow \pi^*$ transitions of the $[\text{PPh}_4]^+$ cation below 300 nm which are not present in the spectrum of **4a**.

The spectrum of **2** in CH_3CN shown in Figure 8 is rather unusual. In the range 320–440 nm a vibronic progression of nine absorption maxima is clearly discernible. The energy difference between two adjacent maxima is constant at $\sim 880 \text{ cm}^{-1}$. The spectrum of **3** measured in pyridine is similar and displays also a vibronic progression but the energy difference is 855 cm^{-1} . The spectrum of electrochemically generated $[\text{Mn}^{\text{VI}}(\text{N})(\text{CN})_4]^-$ in CH_3CN (0.10 M $[\text{N}(n\text{-butyl})_4]\text{PF}_6$) is shown in Figure 9. It is similar to that of **1a** in H_2O containing the isolectronic $[\text{Cr}^{\text{V}}(\text{N})(\text{CN})_4]^{2-}$ anion, but the absorption maxima are red-shifted and the molar extinction coefficients are much larger ($> 1.0 \times 10^3$).

It is notable that the electronic spectra of all complexes $[\text{M}^{\text{V}}(\text{N})(\text{CN})_4(\text{X})]^{n-}$ ($\text{M}^{\text{V}} = \text{Cr}, \text{Mn}$) of idealized C_{4v} symmetry

- (14) (a) Azuma, N.; Ozawa, T.; Tsuboyama, S. *J. Chem. Soc., Dalton Trans.* **1994**, 2609. (b) Groves, J. T.; Takahashi, T.; Butler, W. M. *Inorg. Chem.* **1983**, 22, 884. (c) Buchler, J. W.; Dreher, C.; Lay, K.-L.; Ruap, A.; Gersonde, K. *Inorg. Chem.* **1983**, 22, 879.
- (15) (a) Danopoulos, A. A.; Wilkinson, G.; Sweet, T. K. N.; Hursthouse, M. B. *J. Chem. Soc., Dalton Trans.* **1994**, 1037. (b) Danopoulos, A. A.; Wilkinson, G.; Sweet, T. K. N.; Hursthouse, M. B. *J. Chem. Soc., Dalton Trans.* **1995**, 937.

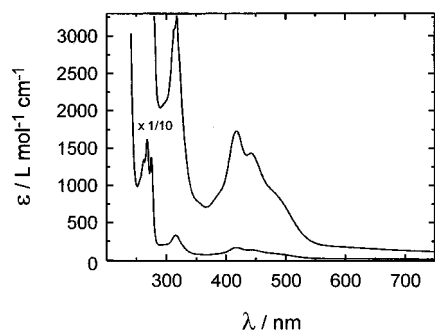
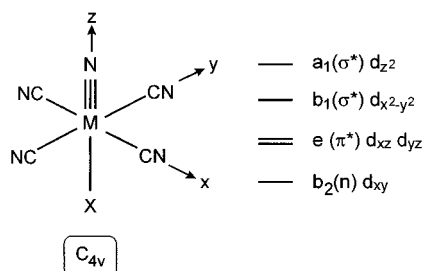


Figure 9. UV-vis spectrum of electrochemically generated $[\text{Mn}^{\text{VI}}(\text{N})(\text{CN})_4]^{2-}$ in CH_3CN (0.10 M $[\text{N}(n\text{-butyl})_4]\text{PF}_6$).

Scheme 2. Ligand-Field Splitting Diagram for an Axially Compressed C_{4v} Complex



are quite similar. They all display two low-intensity d-d transitions which are clearly detectable at >350 nm.

We now describe the electronic structures of these Cr^V (d¹), Mn^{VI} (d¹), and Mn^V (d²) complexes in terms of a ligand-field model developed by Gray et al.¹⁶ (Scheme 2).

In the ground state the formally nonbonding (xy) orbital is half-filled for Cr^V and Mn^{VI} species but filled for Mn^V complexes. The unoccupied $d\pi^*$ levels are degenerate in C_{4v} symmetry and have $\text{M}\equiv\text{N}$ π -antibonding character; the higher-lying ($x^2 - y^2$) and (z^2) orbitals are σ -antibonding.

The energetically lowest-lying spin-allowed transition in the visible region for all complexes is then assigned to a (xy) \rightarrow $d\pi^*$ transition (${}^2\text{B}_2 \rightarrow {}^2\text{E}$ for d¹ (Cr^V and Mn^{VI}) and ${}^1\text{A}_1 \rightarrow {}^1\text{E}$ for d² (Mn^V)). For $[\text{Cr}^{\text{V}}(\text{N})(\text{CN})_4]^{2-}$ in CH_3CN , this is proven by the observation of a vibronic progression ($\Delta\nu = 880$ cm^{-1}). The $\nu(\text{Cr}\equiv\text{N})$ stretching frequency of this anion in the ground state is observed at 1052 cm^{-1} . Promotion of an electron into the antibonding $d\pi^*$ level weakens this bond, and the $\nu(\text{Cr}\equiv\text{N})$ mode of the excited state ${}^2\text{E}$ is lowered to 880 cm^{-1} in **2** and 855 cm^{-1} in **3**. The latter effect clearly shows the influence of the sixth pyridine ligand in trans position relative to the $\text{Cr}\equiv\text{N}$ unit. This is in excellent agreement with the observation that, for the complex $[\text{Fe}^{\text{V}}(\text{N})(\text{tpp})]$, where tpp represents the tetraphenylporphinate dianion, the $\nu(\text{Fe}\equiv\text{N})$ stretch has been observed at 876 cm^{-1} .¹⁷ For this iron(V) (d³) complex, it has been proposed that the antibonding $d\pi^*$ levels are occupied either by two electrons ($S = 3/2$) or by one ($S = 1/2$).

For $[\text{PPh}_4][\text{Mn}(\text{N})(\text{CN})_4]\cdot 2\text{H}_2\text{O}$ in CH_3CN , we have measured the magnetic circular dichroism (MCD) spectrum which is shown in Figure 10. It displays a negative A term centered

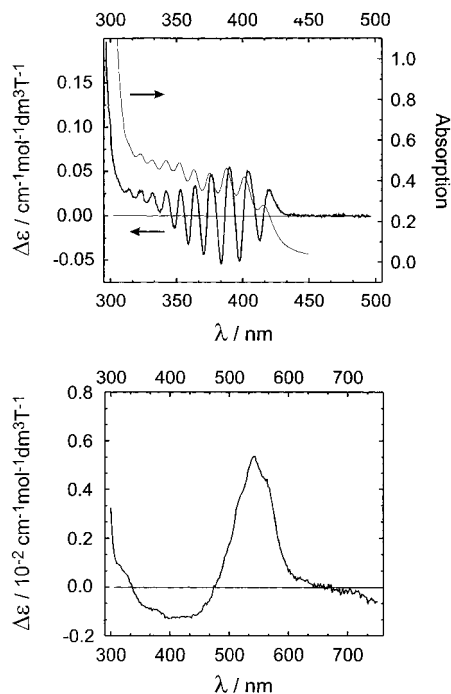


Figure 10. Magnetic circular dichroism spectra of **2** (top) and **5** (bottom) in CH_3CN at 295 K.

with a crossing of the zero-line at 475 nm which proves that the lowest-energy transition is to a degenerate state ($d\pi^*$). We have also measured the MCD spectrum of **2** in acetonitrile, which is shown in Figure 10 (top). Interestingly, each absorption maximum of the vibronic progression displays negative A-term behavior.

The electronic spectra of **4a**, **5**, and **6** (Table 5) clearly indicate that the (xy) \rightarrow (xz), (yz) transition is sensitive to the presence or absence of a sixth ligand in trans position relative to the $\text{M}\equiv\text{N}$ moiety. The five-coordinate species **5** displays absorptions at 350 and 495 nm ($(xy) \rightarrow (x^2 - y^2)$ and $(xy) \rightarrow d\pi^*$, respectively). These maxima are both red-shifted to approximately 365 and 510 nm in **4a** and **6**. We interpret the change in energy of the $d\pi^*$ state as follows: (i) the sixth ligand can behave as a π -acceptor (CN^-) and lowers thereby the energy of the $d\pi^*$ level or (ii) the sixth ligand exerts a structural trans-influence, which would enforce an elongation of the $\text{M}\equiv\text{N}$ bond, thereby decreasing the perturbing strength of the nitrido ligand. Both effects probably contribute.

The fact that the coordination number also has an effect on the energy of the (xy) \rightarrow ($x^2 - y^2$) transition, which in a strong-field approximation is a pure $d_{xy} \rightarrow d_{x^2-y^2}$ transition (O_h symmetry), is then related to the observed flattening of the $\text{Mn}(\text{CN})_4$ moiety on going from five- to six-coordination. This has the effect of raising the energy of the ($x^2 - y^2$) state due to increasing σ -overlap. It is interesting that the (xy) \rightarrow ($x^2 - y^2$) transition has approximately the energy $\Delta\epsilon^{\text{eq}}$, which is the ligand field splitting in homoleptic octahedral hexacyanometalates, $[\text{M}(\text{CN})_6]^{n-}$. Thus it is gratifying that $\Delta\epsilon^{\text{eq}}$ values for $[\text{Ti}(\text{CN})_6]^{3-}$ of 22 800 cm^{-1} ^{18a} and for $[\text{Cr}(\text{CN})_6]^{3-}$ of 26 700 cm^{-1} ^{18b} compare well with 27 000 cm^{-1} for $[\text{Cr}(\text{N})(\text{CN})_5]^{3-}$ or 27 700 cm^{-1} for $[\text{Mn}(\text{N})(\text{CN})_5]^{3-}$.

Discussion

The crystal structure determination of **5** has unequivocally established that a five-coordinate $[\text{Mn}(\text{N})(\text{CN})_4]^{2-}$ anion is

(16) (a) Chang, C. J.; Connick, W. B.; Low, D. W.; Day, M. W.; Gray, H. B. *Inorg. Chem.*, in press. We thank Professor Gray for communicating his results prior to publication. (b) Ballhausen, C. J.; Gray, H. B. *Inorg. Chem.* **1962**, *1*, 111. (c) Winkler, J. R.; Gray, H. B. *J. Am. Chem. Soc.* **1983**, *105*, 1373. (d) Winkler, J. R.; Gray, H. B. *Inorg. Chem.* **1985**, *24*, 346. (e) Miskowski, V. M.; Gray, H. B.; Hopkins, M. D. *Adv. Transition Met. Coord. Chem.* **1996**, *1*, 159.

(17) (a) Wagner, W.-D.; Nakamoto, K. *J. Am. Chem. Soc.* **1989**, *111*, 1590. (b) Wagner, W.-D.; Nakamoto, K. *J. Am. Chem. Soc.* **1988**, *110*, 4044.

(18) (a) Entley, W. R.; Treadway, C. R.; Wilson, S. R.; Girolami, G. S. *J. Am. Chem. Soc.* **1997**, *119*, 6251. (b) Jørgensen, C. K. *Adv. Chem. Phys.* **1963**, *5*, 33.

Table 6. Structurally Characterized Cr^V(N) and Mn^V(N) Complexes

complex	d(M≡N), Å	CN ^a	ν(M≡N), cm ⁻¹ ^b	ref
[Cr(N)(ttp)]	1.565(6)	5	1017	14c
[Cr(N)(bpb)]	1.560(2)	5	1015	20
[Cr(N)L(acac)]ClO ₄	1.575(9)	6	967	5
3	1.570(3)	6	995	this work
[Mn(N)(TpMPP)]	1.515(3)	5	1036	21
[Mn(N)(OEP)]	1.512(2)	5	1050	3c
[Mn(N)(salen)]	1.51	5	1047	9
[Mn(N)(saltmen)]	1.51	5	1047	9
[Mn(N)L(acac)]BPh ₄	1.518(4)	6	983	5
[Mn(N)(3-MeO-sal-Me) ₂]	1.543(4)	5	1047	4
5	1.507(2)	5	1094	this work
6	1.525(4)	6	1041	this work

^a Coordination number. ^b M≡N stretching frequency in the infrared spectrum.

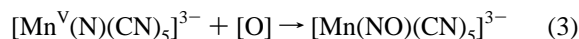
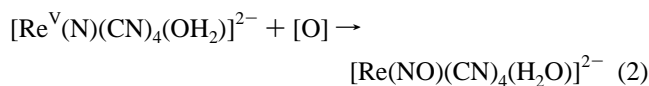
present where the water molecules of crystallization form a hydrogen-bonding network to the terminal nitrogens of coordinated cyano ligands. Two aspects are remarkable: (i) the terminal nitrido ligand is not involved in any hydrogen bonding and (ii) the potential sixth coordination site of the square-base pyramid of the anion is vacant. In contrast, in crystallographically characterized [AsPh₄]₂[Tc(N)(CN)₄(H₂O)]·5H₂O,⁷ the anion is six-coordinate with Tc–N and Tc–OH₂ bond distances at 1.596(10) and 2.559(9) Å, respectively. Similarly, [AsPh₄]₂[Re(N)(CN)₄(H₂O)]·5H₂O^{8b,c} is isostructural (Re–N = 1.639(8) Å, Re–OH₂ = 2.496(7) Å). Interestingly, the M–OH₂ bond length *increases* on going from rhenium to technetium by 0.06 Å whereas at the same time the M–N distance *decreases* by 0.043 Å. In other words, the Re–N bond is slightly less covalent than the corresponding Tc–N bond and then probably much less than the Mn–N bond, which exerts the strongest trans-influence of the series, rendering the water molecule uncoordinated.

On the other hand, reaction of the above series with aqueous NaCN affords the isoelectronic and isostructural six-coordinate anions [M(N)(CN)₅]³⁻ (M = Mn, Re) of which [PPh₄]₃[Re(N)(CN)₅]·7H₂O^{8a} has been structurally characterized. We have solved the crystal structure of [N(CH₃)₄]₂Na[Mn(N)(CN)₅] (**4a**)¹⁹ but found the anions to be severely disordered. Nevertheless, the structure does confirm the atom connectivity of the anion to be [Mn(N)(CN)₅]³⁻, but we refrain from a more detailed discussion of the structure. It reinforces the notion that stronger ligands such as cyanide or pyridine in comparison to water bind to the [M(N)(CN)₄]²⁻ anions (M = Cr, Mn).

Table 6 gives a compilation of all structurally characterized nitrido complexes of Cr^V and Mn^V. In all cases the M≡N bond is extremely short, indicating a significant multiple π-bond character. In fact, the Mn≡N bond in **5** is the shortest reported to date.

We now address an interesting question: To what extent does the formal oxidation of the M≡N group with atomic oxygen affording an M–NO group change the electronic and structural parameters? Consider reactions 2 and 3, where we formally add an oxygen atom to the nitrido complexes. Both nitrosyl complexes have been synthesized and are structurally character-

ized.^{22,23} Common wisdom has it and many textbooks follow



the convention that [M(NO)(CN)₅]³⁻ complexes are formulated with the metal center in the oxidation state +I, e.g. V(I), Cr(I), Mn(I), and Re(I), counting thereby (NO)⁺ as a two-electron σ-donor ligand. The above two nitrido complexes which have also been structurally characterized are invariably assumed to contain an N³⁻ ligand, and as a consequence, the central metal ion is assigned an oxidation state of +V in both cases. As a means for electron bookkeeping, this approach is, of course, legitimate, but it must be kept in mind that the assigned metal oxidation states are formal ones—*without any significant physical meaning*.

This practice is not quite satisfactory because chemists intuitively expect a dramatic structural change between two complexes of similar composition where the formal oxidation states vary by *four* units. For example, the Co–N distances in [Co^{II}(NH₃)₆]²⁺ and [Co^{III}(NH₃)₆]³⁺ change by 0.25 Å—here the oxidation states differ by only *one* unit.²⁴ In contrast, the equatorial M–CN distances in [Re(N)(CN)₄(OH)₂]²⁻^{8c} and [Re(NO)(CN)₄(OH)₂]²⁻²³ are nearly equidistant (average 2.11 and 2.10 Å, respectively). Similarly, this bond length is 2.08 Å in **6** and 1.99 Å in [Mn(NO)(CN)₅]³⁻. More importantly, the observed ν(CN) stretching modes of a given pair of complexes in eqs 2 and 3 are very similar, indicating similar bondings (and electron densities at the central metal ions) in the nitrido *and* corresponding nitrosyl species. These structural results demonstrate how misleading the assignment of formal oxidation states to the metal ions are because the actual electron distributions at the metals cannot be very different in the nitrido and nitrosyl species.

For nitrosyl complexes, this problem has been recognized and alternative electron-counting procedures have been proposed which avoid the assignment of formal oxidation states at the metal ion. The most successful approach is the convention introduced by Enemark and Feltham²⁵ by using the {M–NO}ⁿ formalism where the value of *n* corresponds to the number of d electrons on the metal when the nitrosyl ligand is formally considered to be bound as NO⁺ (2e donor). Both [Mn(NO)(CN)₅]³⁻ and [Re(NO)(H₂O)(CN)₄]²⁻ are then of the type {M–NO}.⁶ We propose here a similar approach for nitrido complexes using the notation {M–N}ⁿ where *n* gives the number of d electrons in this diatomic moiety if the nitrido ligand is formally counted as a trinegatively charged, two-electron donor. Complexes **1–3** would then be of the type {Cr–N}¹, and **4–6** would be of the type {Mn–N}². No assumptions about the actual distribution of electrons between the metal and the NO or nitride group are invoked in either cases.

- (19) Structural data for **4a** (100 K, Mo Kα radiation): orthorhombic space group *Pnma* with *a* = 24.993(5) Å, *b* = 8.577(2) Å, *c* = 9.254(2) Å, and *Z* = 4.
 (20) Che, C.-M.; Ma, J.-X.; Wong, W.-T.; Lai, T.-F.; Poon, C. K. *Inorg. Chem.* **1988**, *27*, 2547.
 (21) Hill, C. L.; Hollander, F. J. *J. Am. Chem. Soc.* **1982**, *104*, 7318.

- (22) (a) Tullberg, A.; Vannerberg, N.-G. *Acta Chem. Scand.* **1967**, *21*, 1462.
 (b) The structure of [Co(en)₃][Mn(NO)(CN)₅]H₂O has also been reported: average Mn–C_{eq} at 1.97 Å, Mn–C_{trans} at 2.02 Å, and Mn–NO at 1.65 Å. Pink, M.; Billing, R. Z. *Kristallogr.* **1996**, *211*, 203.
 (23) Smith, J.; Purcell, W.; Lamprecht, G. J.; Leipoldt, J. G. *Polyhedron* **1995**, *14*, 1795.
 (24) For a discussion of this point and references to the original literature see: Ventur, D.; Wiegardt, K.; Nuber, B.; Weiss, J. Z. *Anorg. Allg. Chem.* **1987**, *551*, 33.
 (25) Enemark, J. H.; Feltham, R. D. *Coord. Chem. Rev.* **1974**, *13*, 339.
 (26) Lyne, P. D.; Mingos, D. M. P. *J. Chem. Soc., Dalton Trans.* **1995**, 1635.

Recently, Lyne and Mingos analyzed the trans-influence in $[\text{Os}(\text{N})\text{X}_5]^{2-}$ ($\text{X} = \text{Cl}, \text{CH}_3, \text{SCH}_3$) in comparison with analogous $[\text{Ru}(\text{NO})\text{X}_5]^{2-}$ complexes in terms of the relative effects of steric and electronic factors and concluded from density functional theory calculations that both factors contribute, but the orbital interaction energy is the major contributor. One of their main conclusions was that “in six-coordinate complexes switching the trans-influencing ligand from a strong π -donor (nitride) to a π -acceptor (nitrosyl) results in an absence of a trans-influence”. Experimentally, this is verified inter alia by the structures of the complexes in eqs 2 and 3. Both nitrido complexes exert a pronounced trans-influence, but for the nitrosyl complexes this effect is absent. In $\text{K}_3[\text{Mn}(\text{NO})(\text{CN})_5] \cdot 2\text{H}_2\text{O}$,²² the $\text{Mn}-\text{C}_{\text{trans}}$ bond is $2.01 \pm 0.01 \text{ \AA}$ and the average $\text{Mn}-\text{C}_{\text{equatorial}}$ bond distance is $1.98 \pm 0.01 \text{ \AA}$, but for isoelectronic $[\text{AsPh}_4]_2[\text{Os}(\text{N})(\text{CN})_5]$,²⁷ these distances are 2.35 and 2.08 \AA , respectively. For the complexes $[\text{Re}(\text{N})(\text{CN})_4(\text{OH}_2)]^{2-}$ and

$[\text{Re}(\text{NO})(\text{CN})_4(\text{OH}_2)]^{2-}$, the situation is similar: the $\text{Re}-\text{OH}_2$ bond distances are 2.496 \AA for the former and only 2.165 \AA for the latter. Note that the $\text{Re}-\text{C}$ distances are identical within experimental error in both complexes.

Acknowledgment. We thank the Danish Research Council for granting the spectropolarimeter and Karen Jørgensen (University Copenhagen) for measuring the MCD spectra. We are grateful to the University of Copenhagen (Chemistry Department) for granting a leave of absence to J.B. Financial support of this work from the Fonds der Chemischen Industrie is also gratefully acknowledged.

Supporting Information Available: Tables of crystallographic and structure refinement data, atom coordinates and U_{eq} values, bond lengths and angles, anisotropic thermal parameters, and calculated and refined positional parameters of hydrogen atoms for complexes **3**, **5**, and **6** (21 pages). Ordering information is given on any current masthead page.

(27) Che, C.-M.; Lam, M. H.-W.; Mak, T. C. W. *J. Chem. Soc., Chem. Commun.* **1989**, 1529.